

Experimental investigation of titanium dioxide as an adsorbent for removal of Congo red from aqueous solution, equilibrium and kinetics modeling

Moussa Abbas

ABSTRACT

The adsorption of Congo red onto titanium dioxide (TiO₂) material has been investigated at batch conditions. The effects of contact time (0–60 min), initial pH (3–11), agitation speed (100–500 rpm), temperature (298–343 K), adsorbent dosage (0.5–2 g/L), and Congo red concentration (5–15 mg/L) on the Congo red adsorption by TiO₂ have been studied. The kinetic parameters, rate constants, and equilibrium adsorption capacities were calculated and discussed for each kinetic model.

The adsorption of Congo red onto TiO₂ is well described by the pseudo-second order equation. The adsorption isotherm follows the Langmuir model, providing a better fit of the equilibrium data. The batch adsorption experiments were carried out to optimize the physical parameters on the Congo red removal efficiency. It has been found that 152 mg/g at 25 °C is removed. The thermodynamic parameters indicate the spontaneous and endothermic nature of the adsorption process with activation energy (E_a) of –64.193 kJ/mol. The positive value of the entropy (ΔS°) clearly shows that the randomness is decreased at the solid–solution interface during the Congo red adsorption onto TiO₂, indicating that some structural exchange may occur among the active sites of the adsorbent and the ions.

Key words | adsorption, Congo red, isotherm, modeling, thermodynamic, titanium dioxide

Moussa Abbas
Laboratory of Soft Technologies and Biodiversity,
Faculty of Sciences,
University M'hamed Bougara of Boumerdes,
Boumerdes 35000,
Algeria
E-mail: moussaiap@gmail.com

HIGHLIGHTS

- The adsorption of Congo red onto titanium dioxide (TiO₂) material has been investigated at batch conditions.
- The equilibrium experimental data were well fitted by the Langmuir isotherm model and it has been found that 152 mg/g at 25°C is removed.
- The adsorption of the dye follows the pseudo-second order kinetic model.
- A thermodynamic study showed the spontaneous and endothermic nature of the adsorption.

INTRODUCTION

Dye production plants and many other industries which utilize dyes are increasing globally by the day with

This is an Open Access article distributed under the terms of the Creative Commons Attribution Licence (CC BY 4.0), which permits copying, adaptation and redistribution, provided the original work is properly cited (<http://creativecommons.org/licenses/by/4.0/>).

doi: 10.2166/wrd.2020.038

advancements in technology (Hameed & Daud 2008). The effluents from textile, leather, food processing, dyeing, cosmetics, paper, and dye manufacturing industries are important sources of dye pollution (Harrache *et al.* 2019a, 2019b). Many dyes and their breakdown products may be toxic for living organisms, in particular, Congo red (Abbas

& Trari 2020a, 2020b). Therefore, decolorizations of dyes are important aspects of wastewater treatment before discharge. It is difficult to remove the dyes from the effluent, because many dyes are carcinogenic and usually yield toxic organic compounds when they biodegrade. In addition, exposure of aquatic species to dye is known to be disastrous as it reduces the dissolved oxygen; hence, there is the need to adopt a holistic approach in removing dyes from industrial effluent before it is discharged into the environment. There are more than 100,000 types of dye commercially available, with over 7×10^5 tons of dyestuff produced annually (Harrache *et al.* 2019a, 2019b). Many treatment processes have been employed for the removal of dyes from industrial effluents. These treatment techniques include ultra filtration (Lakdioui *et al.* 2017), ion exchange membrane (Ran *et al.* 2017), electrochemical degradation (Morsi *et al.* 2011), photo catalytic degradation (Abbas & Trari 2020a, 2020b), and adsorption process (Abbas *et al.* 2016). Among these methods, adsorption of dye onto activated carbon has been the most viable technique (Abbas *et al.* 2019). The growth in industrial and technological advancement globally brought with it the introduction of pollutants of diverse nature into water bodies. Such pollutants include dyes, organic matters, and heavy metals. Their presence in industrial effluents or drinking water is a public health problem due to their absorption and possible accumulation in organisms. Water pollution regulations require textile dye industries to reduce substantially the amount of color in their effluents. Adsorption, as a waste water treatment process, exploits the ability of some solids to concentrate certain substances from solution onto their surface. The most commonly used adsorbent for treatment of textile effluents is activated carbon. However, as the adsorption capacities of the above adsorbents are not large, new adsorbents are still under development. Activated carbons obtained from rubber seed coat, palm seed coat, and apricot stone (Abbas 2020) were investigated for the removal of a wide variety of impurities from water and wastewater. In general, these carbons will be as efficient in the adsorption of both organics and inorganics as the commercial activated carbons. Commercial activated carbons are sophisticated in the sense that they are designed for a variety of applications. If low cost non-conventional sources are used to prepare activated carbons for a specific purpose, then they will be

economical for wastewater treatment. The objective of this study was to investigate the feasibility of using carbonized coir pith for the removal of Congo red, a toxic dye, from wastewater by adsorption method. This study investigated the potential use of titanium dioxide (TiO_2) as an alternative adsorbent for removal of Congo red from wastewater. The effect of factors such as adsorbent dosage, dye concentration, pH, and temperature were experimentally studied to evaluate the adsorption capacity, kinetics, and equilibrium.

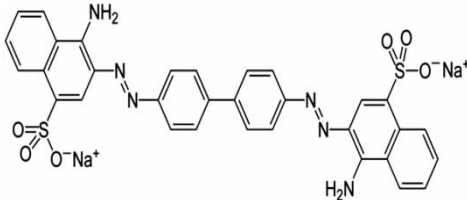
MATERIALS AND METHODS

Adsorbate

The anionic dye used as adsorbate was Congo red bought from Nizochem Laboratory. Congo red has the molecular formula and weight of $\text{C}_{32}\text{H}_{22}\text{N}_6\text{Na}_2\text{O}_6\text{S}_2$ and 696.66 g/mol, respectively (Table 1). H_2SO_4 and NaOH were used to adjust the pH of solution. 100 mg/L of dye solution was prepared by adding 0.1 g of Congo red in 1,000 mL of distilled water, and solutions required for the experimental study were prepared by diluting the CR stock solution to various initial adsorbate concentrations.

Table 1 | General characteristics of Congo red dye

Chemical properties

Brute formula	$\text{C}_{32}\text{H}_{22}\text{N}_6\text{Na}_2\text{O}_6\text{S}_2$
Molecular weight	(696.663 \pm 0.004) g/mol pKa 4
Composition (%)	C: 55.0, N: 12.06, O: 13.78, H: 3.18, Na: 6.60, S: 9.21
Skeletal formula	

Wave number (λ_{max}) 494 nm

Name Congo red

Physical properties

Melting temperature 360 °C

Boiling pressure 760 mmHg

Solubility in water 25 g/L at T = 20 °C

Solubility in alcohol Very soluble

Batch mode adsorption studies

The effects of experimental parameters such as the initial Congo red concentration (5–15 mg/L), pH (2–14), adsorbent dosage (0.5–2 g/L), agitation speed (100–500 rpm), and temperature (298–318 K) on the adsorptive removal of Congo red ions are studied in a batch mode of operation for a specific period of contact time (0–60 min). The Congo red solutions are prepared by dissolving the accurate amount of Congo red (99%) in distilled water, used as a stock solution and diluted to the required initial concentration. pH is adjusted with HCl (0.1 mol/L) or NaOH (0.1 mol/L). For the kinetic studies, the desired quantity of TiO₂ is contacted with 10 mL of Congo red solutions in Erlenmeyer flasks. Then, the flasks are placed on a rotary shaker at 250 rpm and the samples are taken at regular time intervals (5 min) and centrifuged at 3,000 rpm for 10 min. The Congo red content in the supernatant was measured spectrophotometrically on a Perkin Elmer UV-visible spectrophotometer model 550S at a wavelength of 494 nm. The amount of Congo red ions adsorbed by activated carbon q_t (mg/g) is calculated by using the following equation:

$$q_t = \frac{(C_o - C_t) \cdot V}{m} \quad (1)$$

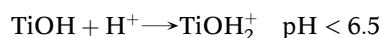
where C_o is the initial Congo red concentration and C_t the Congo red concentration (mg/L) at any time, V the volume of solution (L), and m the mass of TiO₂ (g).

RESULTS AND DISCUSSION

Characterization of TiO₂

The TiO₂ used in this study was a commercial TiO₂ purchased from Ahlstrom (France). It consists of PC500 Titania from Millennium Inorganic Chemicals with a specific surface area 400 m²/g and mean crystallite sizes (5–10 nm). The pH is a parameter that determines the surface properties of solids and the state of the pollutant as a function of its pKa and characterizes the water to be treated. In general, when a compound is partially ionized or

carrying charged functions, it is necessary to consider the electrostatic interactions that occur with TiO₂. Indeed, according to the zero charge point (pHpzc), the surface charge of the solid depends on pH. Thus, for TiO₂, the surface is positively charged below pHpzc (=6.5), and negatively charged above pHpzc (Abbas *et al.* 2018). The reactions of the surface of the TiO₂ are as follows:



The TiO₂ surface is positively charged in acidic solution related to the fixation of protons and negatively in basic medium. The surface charge influences the dye adsorption and, therefore, can promote or limit the adsorption.

Effect of analytical parameters

Spectrum of Congo red in aqueous solution at different pH

The spectrum of the Congo red obtained at pH 7.70 shows the existence of three absorption bands, of unequal intensity and located successively at: 340, 494, and 596 nm (Figure 1). The molar absorption coefficients of these bands are of the order of 15,200 and 21,200, and 29,75 L·mol⁻¹·cm⁻¹, respectively. We also note that the pH influences the behavior of the Congo red, mainly, in an acidic environment (pH = 2.5), where there was a change in the color of the solution, changing from red to purplish blue. Under these conditions, we also noted a widening and a displacement of the most intense band of the spectrum from 500 to 570 nm and a significant reduction in the absorption coefficient which goes to a value of 10,400 L·mol⁻¹·cm⁻¹. To determine the pKa of the acid–base couple of the Congo red, the optical density (OD) was plotted as a function of the pH in the same way as above. To determine the pKa of the acid–base couple of Congo red, the OD was plotted as a function of pH. According to the results reported in Figure 2, the pKa value is 3.6.

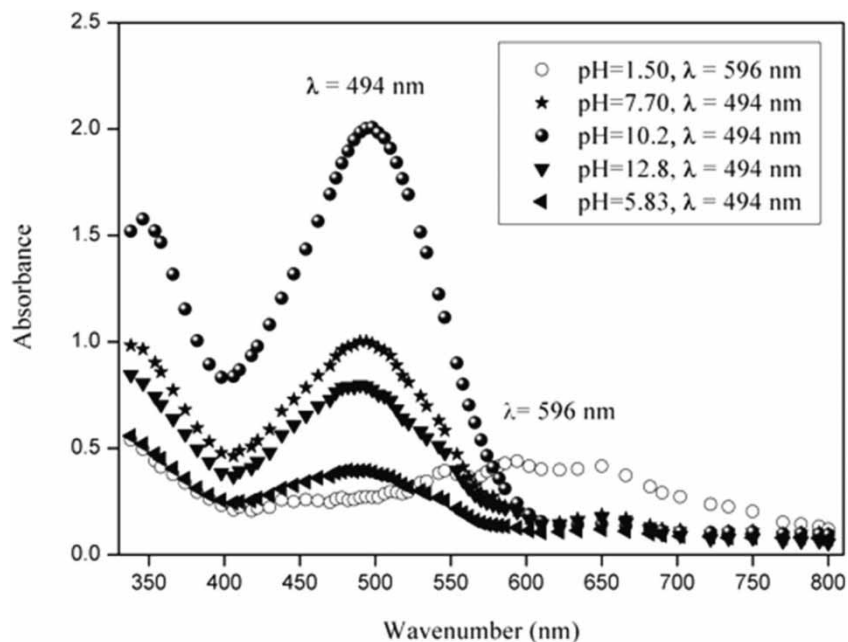


Figure 1 | Spectrum of Congo red in aqueous solution at different pH.

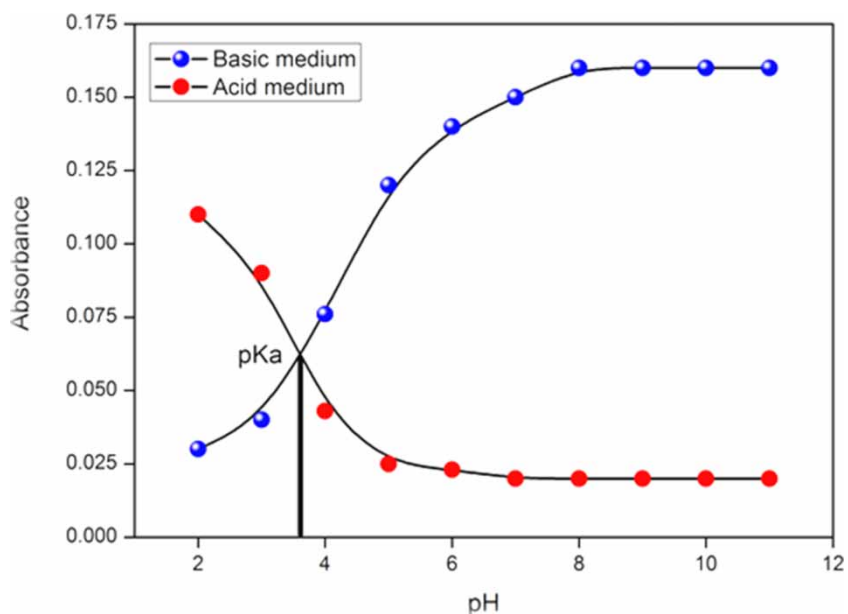


Figure 2 | Change in absorbance at 500 and 655 nm as a function of pH.

Influence of the initial concentration of Congo red on its retention on TiO_2

The study of the adsorption of Congo red on TiO_2 obviously involves determining the contact time, which corresponds

to the adsorption equilibrium or a state of saturation of the support by the substrate. This consists of bringing into contact 10 mg/L of Congo red with 0.1 g/100 mL of TiO_2 . The analysis by UV/visible spectrophotometry will allow the residual concentrations of each substrate to be determined

for the samples taken at different times. Thus, determination of the equilibrium time for the Congo red on the support, will lead to the calculation of the maximum adsorption capacity, which shows that the speed of adsorption is rapid at the start of the process and becomes increasingly slower over time, to finally achieve balance. The adsorption equilibrium time determined is 45 min for Congo red. From the results reported in Figure 3, we note that the increase in the initial concentration of the substrate leads to an increase in the amount adsorbed for the Congo red. The equilibrium time averages 45 min, but for practical reasons, the adsorption experiments are run up to 60 min. With raising the initial Congo red concentration (5–15 mg/L), adsorption increases from 4.5 to 12.5 mg/g. From these results, we can deduce that the adsorption of Congo red onto TiO_2 is done in three stages: fast adsorption of Congo red due to the presence of free sites on the adsorbent surface which translates the linear increase of the adsorption capacity over time; reduction of the adsorption rate, reflected by a small increase in the adsorption capacity attributed to the decrease in the quantity of Congo red in solution and the number of available unoccupied sites. Stability of the adsorption capacity is observed, probably due to the total

occupation of adsorption sites: the establishment of the level therefore reflects this stage. The adsorption capacity of Congo red increases over time to reach a maximum after 45 min and thereafter tends toward a constant value indicating that no more Congo red ions are removed from the solution.

In this case, these results clearly indicate that if the concentration of Congo red in the solution is high, there will be more molecules which will diffuse towards the surface of the sites of the particles of the support, resulting in a significant increase in retention. Similar results were also observed by Tsai *et al.* (2005). We also note that the time required to reach the maximum saturation level is longer for Congo red. This phenomenon is even better perceived for the highest initial concentrations.

Influence of the adsorbent dosage on the retention of Congo red

Figure 4 represents the variation in the adsorbed amounts of the Congo red by varying the initial amount of the adsorbent while keeping the concentration of the dye constant in solution (10 mg/L). The results obtained show that the

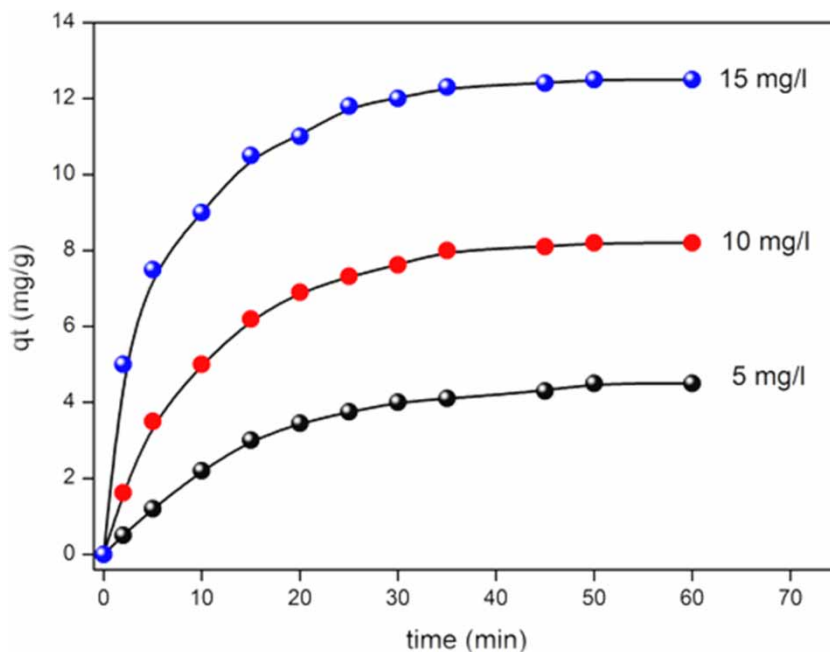


Figure 3 | Influence of the initial concentration of Congo red on its retention on TiO_2 . (adsorbent dosage: 1 g/L, T: 25 °C, pH: 6.60, agitation speed = 250 rpm).

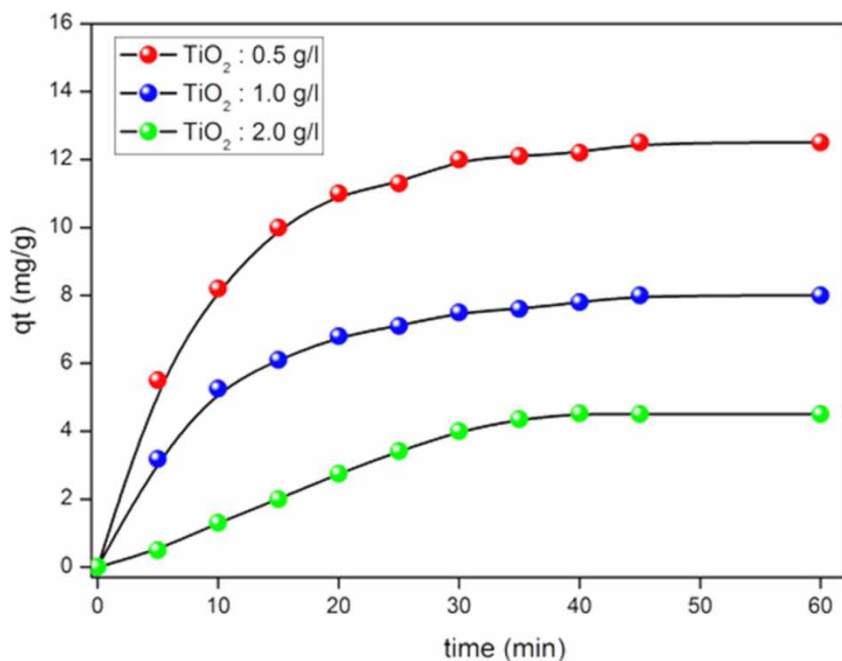


Figure 4 | Influence of the solid/liquid ratio on the retention of Congo red on TiO₂. (CR: 10 mg/L, T: 25 °C, pH: 6.6, stirring speed = 250 rpm).

increase in the mass of the adsorbent in the reaction medium conversely influences the retention capacity and, consequently, the quantity of adsorbed dye. In other words, a reduction in the mass of the support results in a significant improvement in the fixing efficiency. This variation is attributed to an increase in the free surface area of the grains in our adsorbent for low ratios. Indeed, if the mass of the solid in the solution is more and more important, the number of adsorption sites will be too. Consequently, the probability of encountering 'molecule-site' also increases. This will therefore lead to better retention.

Influence of pH on the retention of Congo red on TiO₂

The pH is an important factor for any study in adsorption. It can condition both the surface charge of the adsorbent and the structure of the adsorbate. This parameter also characterizes the waters and its value will depend on the origin of the effluent. In our study, we followed the effect of pH on the absorption of the dye for an initial concentration of Congo red of 10 mg/L and also for a dose of the adsorbent in TiO₂ of 1 g/L. The study of the influence of pH will be considered only in basic medium where no modification on the absorption spectrum of our dye is observed. The

influence of this parameter is studied experimentally, by adjusting the solutions to the desired pH values with NaOH. The curves in Figure 5 show that the increase in the pH of the medium causes a decrease in the amount of adsorbed dye in an alkaline medium. This reduction can be explained both by the chemical state of the TiO₂ surface and by the state of the organic molecule which is ionizable at this pH. It is well known that for pH values higher than that of the zero charge point (pHpzc), for example, at pH = 6.5, the surface becomes negatively charged for TiO₂ (Hu *et al.* 2003). However, for higher pH values, Congo red with two sulfonic groups, ionizes more easily and therefore becomes a soluble anion. Under these conditions, it is far from the surface negative of TiO₂, resulting in a decrease in its retention capacity.

Influence of the agitation speed on the retention of Congo red on TiO₂

The results of the variation in the speed of agitation on the retention of Congo red are shown in Figure 6. From this representation, it can be seen that the retention capacity of the dye Congo red increases slightly as a function of the speed of agitation. These results can be explained by the fact that the

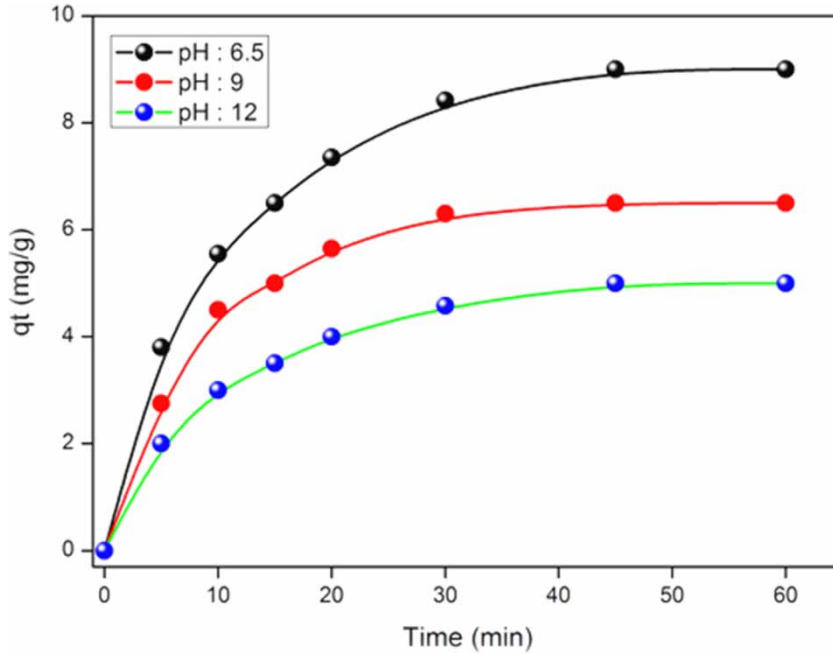


Figure 5 | Influence of pH on the retention of Congo red on TiO_2 . (CR: 10 mg/L, T: 25 °C, stirring speed = 250 rpm).

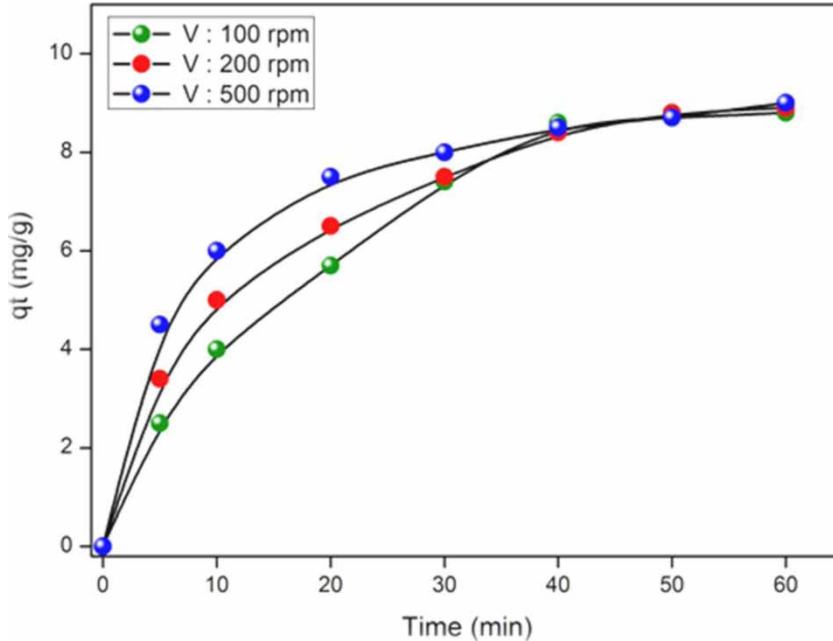


Figure 6 | Influence of the agitation speed on the retention of Congo red on TiO_2 . (CR: 10 mg/L, T: 25 °C, pH: 6.6, stirring speed = 250 rpm).

increase acts favorably on the probability of contact of the substrate with the support, by creating a zone of turbulence. Furthermore, the reduction in the thickness of the boundary layer around the adsorbent particles is attributed to the

increase in the phenomenon, known as 'mixing' (Weeks & Rabani 1966), thus promoting the process of adsorption. These results are in agreement with those of Ho & Chiang (2001).

Influence of temperature on the retention of Congo red on TiO₂

Experience has shown that temperature has two major effects on the adsorption process, as shown in Figure 7. The first, linked to an increase in temperature, promotes the diffusion of molecules through the outer boundary layer and the internal pores of the particles of the adsorbent (decrease in the viscosity) while the second, always linked to the increase in temperature, can affect the adsorption capacity. This, therefore, leads to the quantities of Congo red indicating that the increase in temperature promotes the retention of the dye (Al-qodah 2000).

Adsorption of Congo red onto TiO₂

Adsorption kinetic study

The kinetic study is important since it describes the uptake rate of adsorbate, and controls the residual time of the whole process. Several models have been proposed to study the mechanisms controlling the adsorption. In this study, the experimental data of Congo red adsorption are examined

using a pseudo-first and pseudo-second order kinetic model. The pseudo-first order equation (Lagergren 1998) is given as:

$$\log(q_e - q_t) = \log q_e - \frac{K_1}{2.303} \cdot t \quad (2)$$

The pseudo-second order model (Ho & McKay 1998) is expressed as:

$$\frac{t}{q_t} = \frac{1}{K_2 \cdot q_e^2} + \frac{1}{q_e} \cdot t \quad (3)$$

where q_t (mg/g) is the amount of Congo red adsorbed on TiO₂ at the time t (min). K_1 (min⁻¹) and K_2 (g/mg·min) are the pseudo-first order and pseudo-second order kinetics constants, respectively. The slope and intercept of the plots $\ln(q_e - q_t)$ versus t and t/q_e versus t were used to determine the first-order rate constants K_1 and q_e and second-order rate constants K_2 and q_e , respectively.

The rate constants predict the uptakes and the corresponding correlation coefficients for TiO₂ are summarized in Table 2. For the pseudo-first order kinetic (Figure 8), the experimental data deviate from linearity, as evidenced from the low values of q_e and C_o

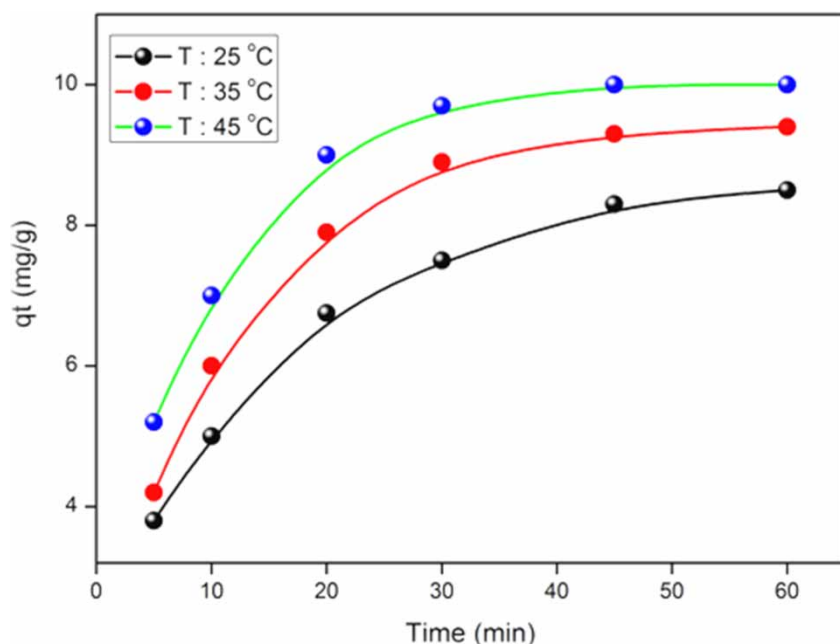
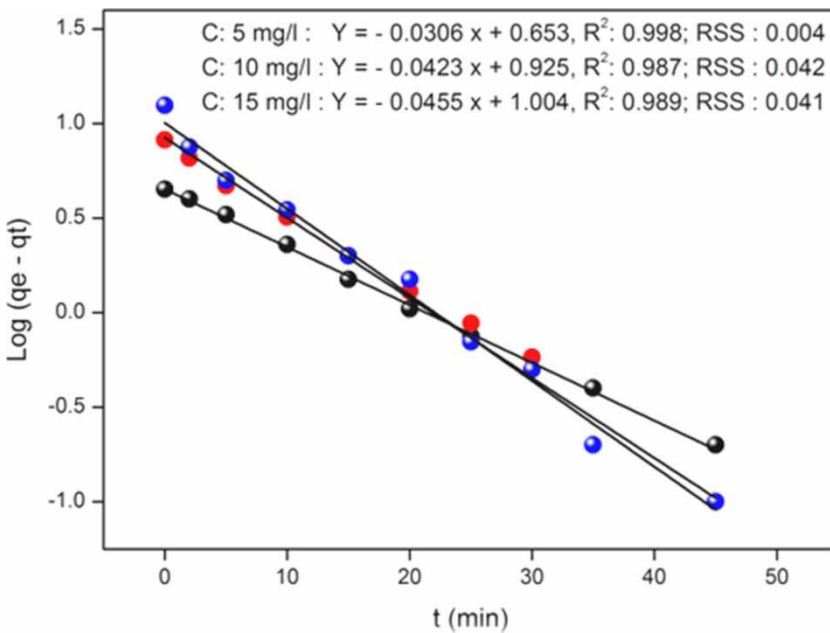


Figure 7 | Influence of temperature on the retention of Congo red on TiO₂ (CR: 10 mg/L, T: 25 °C, pH: 6.6, stirring speed = 250 rpm).

Table 2 | Pseudo-first order, pseudo-second order, Elovich, and intraparticle diffusion model constants and correlation coefficients for (CR) adsorption onto TiO₂

Second order					Pseudo-first order				
C _o (mg/L)	q _{ex} (mg/g)	q _{cal} (mg/g)	R ²	SSE	K ₂ (g/mg·mn)	q _{cal} (mg/g)	R ²	SSE (%)	K ₁ (mn ⁻¹)
5	4.50	6.097	0.981	1.658	0.0913	4.497	0.9989	0.004	0.0071
10	8.20	9.615	0.997	0.100	0.0122	8.414	0.997	0.042	0.0974
15	12.50	13.51	0.999	0.016	0.0185	10.09	0.989	0.041	0.1047

Elovich				Diffusion			
C _o (mg/L)	R ²	β (g/mg)	α (mg/g·mn)	SSE	K _{in} (mg/g·mn ^{1/2})	R ²	C (mn ^{1/2})
5	0.982	0.772	0.830	0.309	0.243	0.90	2.68
10	0.0978	0.484	1.729	0.955	0.233	0.69	6.48
15	0.968	0.432	8.484	1.690	0.206	0.74	10.98

**Figure 8** | First order kinetic plot for the adsorption of Congo red on TiO₂.

and the model is inapplicable for the present system. By contrast, the correlation coefficient and $q_{e,cal}$ determined from the pseudo-second order kinetic model agree with the experimental data (Figure 9) and its applicability suggests that the adsorption of Congo red onto TiO₂ is based on chemical reaction (chemisorption), involving an exchange of electrons between adsorbent and adsorbate.

The Elovich kinetic equation is related to the chemisorptions process (Figure 10) and is often validated for systems where the surface of the adsorbent is heterogeneous (Juang & Chen 1997); the linear form is given by:

$$q_t = \left(\frac{1}{\beta}\right) \ln \alpha \cdot \beta + \left(\frac{1}{\beta}\right) Lnt \quad (4)$$

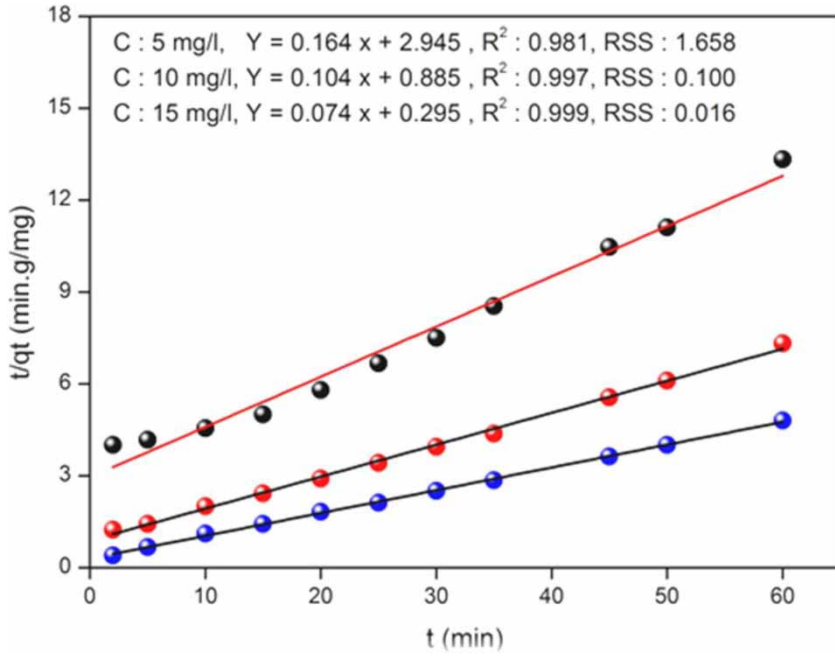


Figure 9 | Pseudo-second order kinetic plot for the adsorption of Congo red on TiO₂.

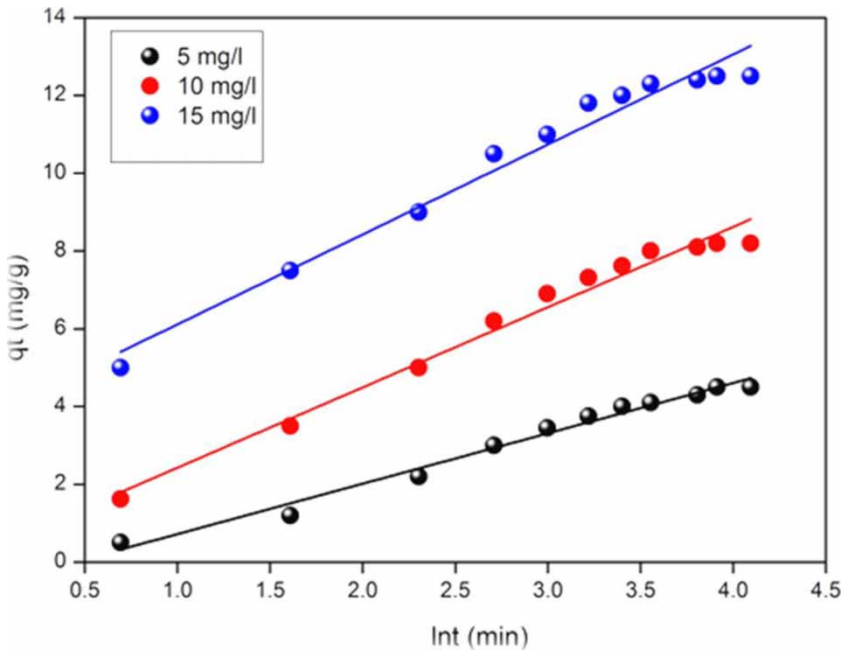


Figure 10 | Elovich kinetic plot for the adsorption of Congo red on TiO₂.

where α (mg/g·min) is the initial adsorption rate, and β (mg/g) the relationship between the degree of surface

coverage and the activation energy involved in the chemisorption.

Intra-particle diffusion equation

The possibility of intra-particle diffusion during the transportation of adsorbate from solution to the particles' surface was also investigated by using the intra-particle diffusion model given by the following formula (Weber & Morris 1963):

$$q_t = K_{in} \sqrt{t} + C \quad (5)$$

where K_{in} is the intra-particle diffusion rate constant ($\text{mg/g min}^{1/2}$), q_t the amount of Congo red adsorbed at time t and C (mg/g) the intercept. A plot of q_t versus $t^{1/2}$ enables determination of both K_{in} and C . Figure 11 present a multi-linearity correlation, which indicates that two steps occur during the Congo red adsorption. The mechanism of adsorption is complex but the intra-particle diffusion is important in the early stages. The first linear portions could be due to intra-particle diffusion effects. The slopes of the linear parts are defined as rate parameters, characteristic of the adsorption rate in the region where the intra-particle diffusion occurs. Initially, and within a short-time period, it is postulated that Congo red is transported to the

adsorbent external surface through the film diffusion with a high rate. After saturation of the surface, the Congo red ions enter inside adsorbent by intra-particle diffusion through the pores and internal surface diffusion until equilibrium is reached, which is represented by the second straight lines. The constants of the different models deduced after modeling are grouped in Table 2.

Adsorption equilibrium isotherms

To assess the performance of adsorbent, different equations and isotherms exist, out of which, the Langmuir (1918), Freundlich (1906), Temkin (Temkin & Pyzhev 1940), and Elovich (Ghaedj *et al.* 2013) isotherms were used and are presented in Figure 12. In addition, the isotherm models were applied at optimal conditions of the parameters. The Langmuir model is the best known and most widely applied, and it is represented by the non-linear and linear forms:

$$q_e = \frac{q_{max} \cdot K_L \cdot C_e}{1 + K_L \cdot C_e}$$

$$\frac{1}{q_e} = \frac{1}{q_{max}} + \frac{1}{q_{max} \cdot K_L \cdot C_e} \quad (6)$$

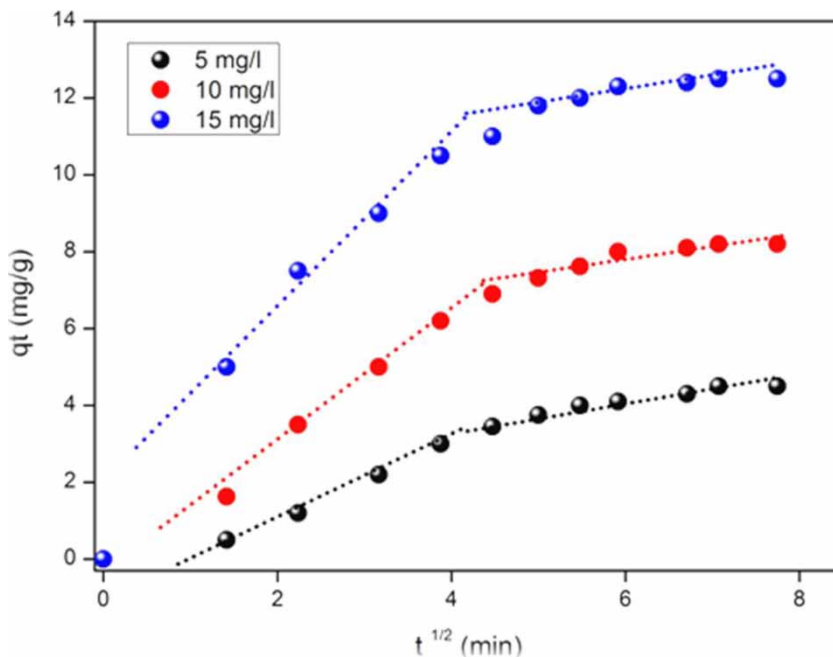


Figure 11 | Application of intra-particle diffusion for the adsorption of Congo red on TiO_2 .

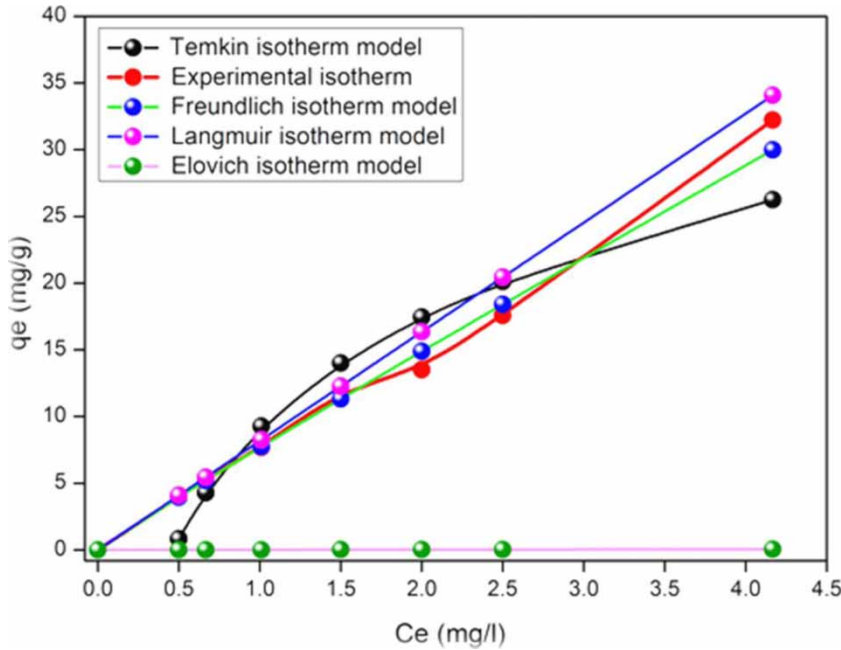


Figure 12 | Adsorption isotherms of the different models under optimal conditions.

where C_e is the equilibrium concentration (mg/L), q_{max} the monolayer adsorption capacity (mg/g), and K_L the constant related to the free adsorption energy (L/mg). The applicability to the adsorption is compared by evaluating the statistic RSE values at 25 °C. The smaller RSE values obtained for the models indicate a better fitting. The essential features of the Langmuir are

$$R_L = \frac{1}{1 + K_L \cdot C_0} \tag{7}$$

where C_0 is the initial concentration of the adsorbate in solution. R_L indicates the type of isotherm: irreversible ($R_L = 0$), favorable ($0 < R_L < 1$), linear ($R_L = 1$), or unfavorable ($R_L > 1$). In this study, the R_L values are smaller than 1, thus confirming that the adsorption is favored in both cases as well as the applicability of the Langmuir isotherm. The Freundlich isotherm is valid for non-ideal adsorption on heterogeneous surfaces as well as multilayer sorption:

$$q_e = K_F \cdot C_e^{1/n}$$

$$\ln q_e = \ln K_F + \frac{1}{n} \cdot \ln C_e \tag{8}$$

The constant K_F characterizes the adsorption capacity of the adsorbent (L/g) and n an empirical constant related to the magnitude of the adsorption driving force. Therefore, a plot $\ln q_e$ versus $\ln C_e$ enables the determination of both the constant K_F and n . The Temkin isotherm describes the behavior of adsorption systems on heterogeneous surfaces, and is applied in the following form:

$$q_e = (RT/b) \cdot \ln(ACe)$$

$$q_e = B_T \ln C_e + B_T \ln A_T \tag{9}$$

The adsorption data are analyzed according to Equation (8). Therefore, the plot versus q_e versus $\ln C_e$ enables the determination of the constants A_T and B_T . The Elovich isotherm is based on the principle of the kinetic, assuming that the number of adsorption sites augments exponentially with the adsorption; this implies a multilayer adsorption described by:

$$\frac{q_e}{q_{max}} = K_E \cdot C_e \cdot \exp\left(-\frac{q_e}{q_{max}}\right)$$

$$\ln \frac{q_e}{C_e} = \ln(q_m \cdot K_E) - \frac{q_e}{q_{max}} \tag{10}$$

where K_E (L/mg) is the Elovich constant at equilibrium, q_{max} (mg/g) the maximum adsorption capacity, q_e (mg/g) the adsorption capacity at equilibrium, and C_e (g/L) the concentration of the adsorbate at equilibrium. Both the equilibrium constant and maximum capacity are calculated from the plot of $\ln(q_e/C_e)$ versus q_e . The constants of the different models deduced after modeling are grouped in Table 3.

Error analysis

An error is required to evaluate the fit of an isotherm equation to the experimental equilibrium data obtained. In this study, the linear and non-linear (Langmuir, Freundlich, Temkin, and Elovich isotherm models) coefficients of determination (R^2) and RSE (X^2) (residual sum of errors) test were performed for all the isotherm models. The RSE test statistic is basically the sum of the squares of the differences between the experimental data and the data obtained by calculating from models, with each squared difference divided by the corresponding data calculated using the models. This can be represented mathematically as:

$$X^2 = \sum_1^N \frac{(q_{e,exp} - q_{e,cal})^2}{q_{e,cal}} \quad (11)$$

where $q_{e,cal}$ is the equilibrium capacity obtained by calculating from the model (mg/g) and $q_{e,exp}$ is the experimental data of the equilibrium capacity (mg/g).

Thermodynamic properties' modeling studies

The thermodynamic properties were investigated to determine whether the adsorption process occurred

spontaneously. The thermodynamic parameters, namely, standard enthalpy (ΔH° , kJ/mol), standard entropy (ΔS° , J/mol K), and standard free energy (ΔG° , kJ/mol), were calculated using the following equations (Li *et al.* 2010):

$$\Delta G^\circ = \Delta H^\circ - T\Delta S^\circ \quad (12)$$

$$\Delta G^\circ = -RT \ln K_d \quad (13)$$

$$K_d = \frac{q_e}{C_e} \quad (14)$$

$$\ln K_d = -\frac{\Delta H^\circ}{RT} + \frac{\Delta S^\circ}{R} \quad (15)$$

where R is the gas constant (8.314 J/mol K), T (K) is temperature where K_d is the distribution coefficient, q_e (mg/g) is the quantity of Congo red adsorbed at equilibrium, and C_e (mg/L) is the quantity of Congo red remaining in solution at equilibrium. The thermodynamic equilibrium constant K_d for the sorption was determined by plotting q_e/C_e versus C_e and extrapolating to zero q_e . The ΔH° and ΔS° values obtained from the slope and intercept of van 't Hoff plots of $\ln K$ versus $1/T$ and the ΔG° values at various temperatures are summarized in Table 4.

The adsorption capacity of Congo red increases with raising temperature in the range 293–328 K:

$$\ln K_2 = \ln A - \frac{E_a}{RT} \quad (16)$$

A pre-exponential factor, E_a the activation energy, and K_2 (g/mg·min) is the pseudo-second order kinetics constant at different temperatures. The energy ($E_a = -64.193$ kJ/mol)

Table 3 | Sorption isotherm coefficients of different models

25 °C	Langmuir	Freundlich	Temkin	Elovich
K_L	0.0538 L/mg	$1/n$: 0.955	B : 11.991	K_E : 0.013 L/mg
q_{max}	152 mg/g	n : 1.047	A_T : 2.144 L/mg	q_{max} : 613 mg/g
		K_F : 7.675 mg/g	ΔQ : 31.414 kJ/mol	
R^2	0.996	0.992	0.838	0.134
RSE	0.0001	0.021	75.91	0.26

RSE: residual sum of errors, R^2 : determination coefficient, ΔQ : Temkin energy.

Table 4 | Thermodynamic parameters for the CR adsorption onto TiO₂

T (K)	1/T (K ⁻¹)	(q _e /C _e) = f(C _e)	K	LnK	ΔH° (kJ/mol)	ΔS° (J/K·mol)	ΔG° (J/mol)
293	0.003413	R ² : 0.997	0.2326	-1.458	10.79254	24.759	-3,538.15
308	0.003247	R ² : 0.997	0.2924	-1.229			-3,166.76
318	0.003145	R ² : 0.994	0.3317	-1.104			-2,919.18
328	0.003049	R ² : 0.996	0.3733	-0.985			-2,671.58

can be obtained by plotting $\ln K_2$ against the reciprocal of the absolute temperature T (Figure 13).

Performance of the prepared ASAC

In order to have an idea about the efficiency of the TiO₂, a comparison of basic dye adsorption of this work and other relevant studies is reported in Table 5. The adsorption capacity of the adsorbent q_{max} is the parameter used for the comparison. One can conclude that the value of q_{max} is in good agreement with those of most previous works, suggesting that Congo red could be easily adsorbed on TiO₂ used in this work.

CONCLUSION

This study has shown that TiO₂ can be employed as an effective adsorbent for the removal of Congo red from aqueous solution. The Freundlich and Langmuir isotherm models provided a better fit of the equilibrium adsorption data giving a maximum adsorption capacity of 152 mg/g at a temperature of 25 °C. The pseudo-second order model proved the best description of the kinetic data. The negative value of ΔG° and positive value of ΔH° indicate that the adsorption of Congo red onto TiO₂ is spontaneous and endothermic over the studied range of temperatures.

The positive value of ΔS° demonstrated clearly that the randomness increased at the solid-solution interface during the Congo red adsorption onto TiO₂, indicating

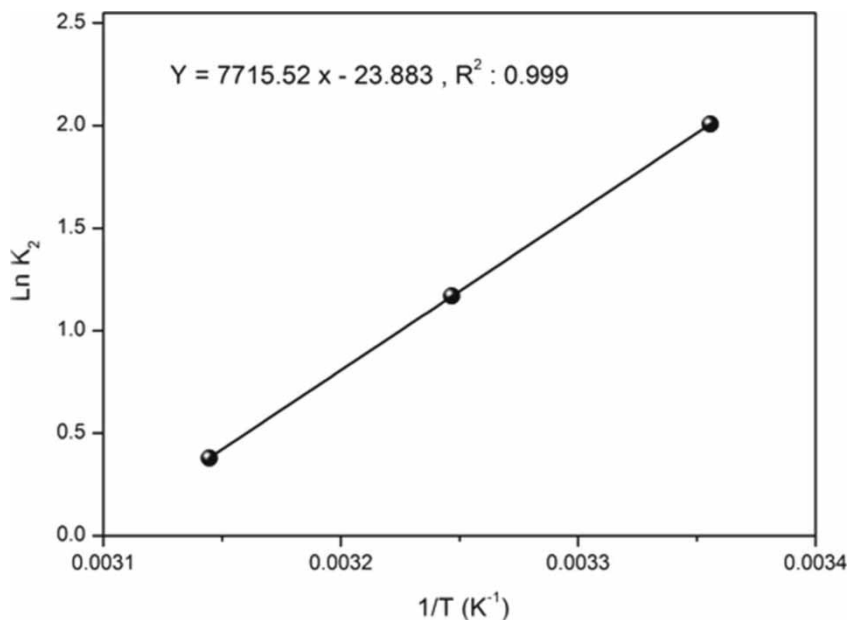
**Figure 13** | Determination of activation energy for the adsorption of Congo red on TiO₂.

Table 5 | Adsorption capacities of Congo red by various adsorbents

Adsorbent	q_m (mg/g)	Reference
Apricot stone activated carbon (ASAC)	32.852	Abbas & Trari (2015)
Apricot stone activated carbon (ASAC)	23.42	Abbas & Trari (2015)
Waste red mud	4.04	Gupta <i>et al.</i> (1990)
Mixed adsorbent fly ash and coal	44.00	Namasivayam <i>et al.</i> (1996)
Waste orange peel	22.44	Namasivayam & Kanchana (1993)
Waste banana pith	9.50	Lian <i>et al.</i> (2009)
Ca-bentonite	107.41	Namasivayam & Kavitha (2002)
Coir pith	6.70	Namasivayam <i>et al.</i> (1994)
Waste Fe(III)/Cr(III) hydroxide	1.01	Bouchamel <i>et al.</i> (2011)
Activated carbon (Zn CO ₂) 800	35.21	Sumanjit <i>et al.</i> (2013)
Activated carbon (Zn 600, CO ₂ 800)	30.22	Sumanjit <i>et al.</i> (2013)
Ground nut shells charcoal	117.6	Cotoruelo <i>et al.</i> (2010)
<i>Eichornia</i> charcoal	56.80	Cotoruelo <i>et al.</i> (2010)
Lignin-based activated carbons	812.5	Ozman & Yilmaz (2007)
TiO₂ semiconductor	152	This study

that some structural exchange may occur among the active sites of the adsorbent and the ions.

The adsorption of Congo red ions by TiO₂ follows a pseudo-second order kinetic model, which relies on the assumption that chemisorptions may be the rate-limiting step. In chemisorption, the Congo red ions are attached to the adsorbent surface by forming a chemical bond and tend to find sites that maximize their coordination number with the surface. The value of q_{max} is in good agreement with those of most previous works, suggesting that Congo red could be easily adsorbed on TiO₂ used in this work.

This study in a tiny batch gave rise to encouraging results, and we wish to achieve adsorption tests in column mode under the conditions applicable to the treatment of industrial effluents. The present investigation showed that TiO₂ is a potentially useful adsorbent for metals, acid, and basic dyes.

ACKNOWLEDGEMENTS

Financial support for the work was provided by Boumerdes University, Science Faculty, Chemical Department. The author attests that there is no conflict of interest and financial, personal, or other relationships with other people, laboratories, or organizations worldwide.

DATA AVAILABILITY STATEMENT

Data cannot be made publicly available; readers should contact the corresponding author for details.

REFERENCES

- Abbas, M. 2020 Experimental investigation of activated carbon prepared from apricot stones material (ASM) adsorbent for removal of malachite green (MG) from aqueous solution. *Adsorpt. Sci. Technol.* **38** (1–2), 24–45.
- Abbas, M. & Trari, M. 2015 Kinetic, equilibrium and thermodynamic study on the removal of Congo red from aqueous solutions by adsorption onto apricot stone. *Process Saf. Environ. Prot.* **98**, 424–436.
- Abbas, M. & Trari, M. 2020a Photocatalytic degradation of Asucryl Red (GRL) in aqueous medium on heat-treated TiO₂ powder – effect of analytical parameters and kinetic modeling. *Desalin. Water Treat.* **180**, 398–404.
- Abbas, M. & Trari, M. 2020b Removal of Methylene Blue (MB) in aqueous solution by economic adsorbent derived from apricot stone activated carbon (ASAC). *Fibers Polym.* **21** (4), 810–820.
- Abbas, M., Abdelhamid, C., Samia, K. & Aksil, T. 2016 Adsorption in simple batch experiments of Coomassie blue G-250 by apricot stone activated carbon – kinetics and isotherms modeling. *Desalin. Water Treat.* **57** (32), 15037–15048.
- Abbas, M., Aksil, T. & Trari, M. 2018 Removal of toxic methyl green (MG) in aqueous solutions by apricot stone activated

- carbon – equilibrium and isotherms modeling. *Desalin. Water Treat.* **125**, 93–101.
- Abbas, M., Harrache, Z. & Trari, M. 2019 Removal of gentian violet in aqueous solution by activated carbon equilibrium, kinetics, and thermodynamic study. *Adsorpt. Sci. Technol.* **37** (7–8), 566–589.
- Al-qodah, Z. 2000 Adsorption of dyes using shale oil ash. *Water Res.* **34** (17), 4295–4303.
- Bouchamel, N., Merzougui, Z. & Addoun, F. 2011 Adsorption in aqueous medium of two dyes on activated carbon based on date nuclei. *J. Soc. Algér. Chimie* **21** (1), 1–14.
- Cotoruelo, L. M., Marqués, M. D., Díaz, F. J., Rodríguez-Mirasol, J., Rodríguez, J. J. & Cordero, T. 2010 Equilibrium and kinetic study of Congo red adsorption onto lignin-based activated carbons. *Transp. Porous Media* **83**, 573–590.
- Freundlich, H. 1906 Concerning adsorption in solutions. *Z. Phys. Chem. Stoch.* **57**, 385–470.
- Ghaedj, M., Karimi, F., Barrazzch, B., Sahraei, R. & Danichfar, A. 2013 Removal of Reactive Orange 12 from aqueous solutions by adsorption on tin sulfide nanoparticle loaded on activated carbon. *J. Ind. Eng. Chem.* **19** (3), 756–763.
- Gupta, G. S., Prasad, G. & Sing, V. N. 1990 Removal of Chrom dye from aqueous solution by mixed adsorbents: fly ash coal. *Water Res.* **24**, 45–50.
- Hameed, B. H. & Daud, F. B. M. 2008 Adsorption studies of basic dye on activated carbon derived from agricultural waste: Hevea brasiliensis seed coat. *Chem. Eng. J.* **139**, 48–55.
- Harrache, Z., Abbas, M., Aksil, T. & Mohamed, T. 2019a Thermodynamic and kinetics studies on adsorption of Indigo Carmine from aqueous solution by activated carbon. *Microchem. J.* **144**, 180–189.
- Harrache, Z., Abbas, M., Aksil, T. & Trari, M. 2019b Modeling of adsorption isotherms of (5, 5'-disodium indigo sulfonate) from aqueous solution onto activated carbon: equilibrium, thermodynamic studies, and error analysis. *Desalin. Water Treat.* **147**, 273–283.
- Ho, Y. S. & Chiang, C. C. 2001 Sorption studies of acid dye by mixed sorbents. *Adsorption* **7**, 139–147.
- Ho, Y. S. & McKay, G. 1998 Kinetic models for the sorption of dye from aqueous solution by wood. *J. Environ. Sci. Health B* **76** (4), 183–191.
- Hu, C., Tang, Y., Yu, J. C. & Wong, P. K. 2003 Photocatalytic degradation of cationic blue X-GRL adsorbed on TiO₂/SiO₂ photocatalyst. *Appl. Catal. B: Environ.* **40** (2), 131–140.
- Juang, R. S. & Chen, M. L. 1997 Application of the Elovich equation to the kinetics of metal sorption with solvent-impregnated resins. *Ind. Eng. Chem. Res.* **36**, 813–820.
- Lagergren, S. 1998 About the theory of so-called adsorption of soluble substance. *Kung. Sven. VetenHand* **24**, 1–39.
- Lakdioui, T., Essamri, A. & El Harfi, A. 2017 Optimization study of ultrafiltration rate of a membrane based on polysulfone modified titanium dioxide on coloured water by indigo. *J. Mater. Environ. Sci.* **8** (11), 4052–4056.
- Langmuir, I. 1918 The adsorption of gases on plane surfaces of glass, mica and platinum. *J. Am. Chem. Soc.* **40**, 1361–1403.
- Li, Q., Yue, Q., Su, Y., Gao, B. & Sun, H. 2010 Equilibrium, thermodynamics and process design to minimize adsorbent amount for the adsorption of acid dyes onto cationic polymer-loaded bentonite. *Chem. Eng. J.* **158**, 489–497.
- Lian, L., Guo, L. & Guo, C. 2009 Adsorption of Congo red from aqueous solutions onto Ca-bentonite. *J. Hazard. Mater.* **161** (1), 126–131.
- Morsi, M. S., Al-Sarawy, A. A. & Shehab Eldein, W. A. 2011 Electrochemical degradation of some organic dyes by electrochemical oxidation on a Pb/PbO₂ electrode. *Desalin. Water Treat.* **26**, 301–308.
- Namasivayam, C. & Kanchana, N. 1993 Removal of Congo red from aqueous solutions by cellulosic waste banana pith. *Pertanica J. Sci. Technol.* **1**, 32–42.
- Namasivayam, C. & Kavitha, D. 2002 Removal of dyes from aqueous solutions by adsorption onto activated carbon prepared from coir pith, an agricultural solid waste. *Dyes Pigment.* **54**, 47–58.
- Namasivayam, C., Jeya Kumar, R. & Yamuna, R. T. 1994 Dyes removal from wastewater by adsorption on waste Fe(III)/Cr(III). *Waste Manage.* **14**, 643–648.
- Namasivayam, C., Muniasamy, N., Gaytri, K., Rani, M. & Ranganathan, K. 1996 Removal of dyes from aqueous solutions by cellulosic waste orange peel. *Bioresour. Technol.* **57** (1), 37–43.
- Ozman, E. Y. & Yilmaz, M. 2007 Use of β -cyclodextrin and starch based polymer for sorption of Congo red from aqueous solutions. *J. Hazard. Mater.* **148**, 303–310.
- Ran, J., Wu, L., He, Y., Yang, Z., Wang, Y., Jiang, C., Ge, L., Bakangura, E. & Xu, T. 2017 Ion exchange membranes: new developments and application. *J. Membr. Sci.* **522** (15), 267–291.
- Sumanjit, K., Seema, R. & Rakesh Kumar, M. 2013 Adsorption kinetics for the removal of hazardous dye Congo red biowaste materials as adsorbents. *J. Chem.* <http://dx.doi.org/10.1155/2013/628582>.
- Temkin, M. & Pyzhev, V. 1940 Kinetics of ammonia synthesis on promoted iron catalysts. *Acta Physicochem. URSS* **12**, 327–356.
- Tsai, W. T., Chang, Y. M., Lai, C. W. & Lo, C. C. 2005 Adsorption of ethyl violet dye in aqueous solution by regenerated spent bleaching earth. *J. Colloid Interface. Sci.* **289**, 333–338.
- Weber, M. J. & Morris, J. 1963 Kinetic of adsorption on carbon from solution. *ASCE J. Saint Eng. Div.* **89**, 31–51.
- Weeks, J. L. & Rabani, J. 1966 The pulse radiolysis of deaerated carbonate solutions, transient optical spectrum and mechanism, pK or OH radicals. *J. Phys. Chem.* **82**, 138–141.